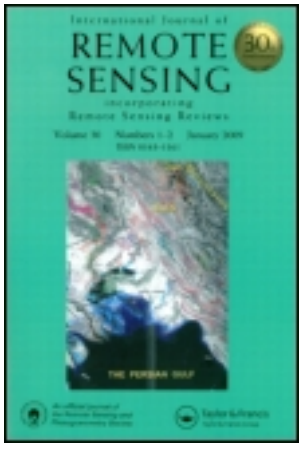

International Journal of Remote Sensing

Publication details, including instructions for authors and subscription information:
http://www.tandfonline.com/loi/tres20

Assessment of land surface temperature in relation to landscape metrics and fractional vegetation cover in an urban/peri-urban region using Landsat data

Youshui Zhang [a b], Inakwu O.A. Odeh [b] & Elnazir Ramadan [c]

[a] College of Geography, Fujian Normal University, Fuzhou, 350007, China

[b] Faculty of Agriculture, Food and Natural Resources, The University of Sydney, Sydney, NSW 2006, Australia

[c] Faculty of Arts and Sciences, Qatar University, Doha, 2713, Qatar

Version of record first published: 10 Sep 2012.

To cite this article: Youshui Zhang, Inakwu O.A. Odeh & Elnazir Ramadan (2013): Assessment of land surface temperature in relation to landscape metrics and fractional vegetation cover in an urban/peri-urban region using Landsat data, International Journal of Remote Sensing, 34:1, 168-189

To link to this article: http://dx.doi.org/10.1080/01431161.2012.712227

International Journal of Remote Sensing
Vol. 34, No. 1, 10 January 2013, 168–189

Taylor & Francis
Taylor & Francis Group

Assessment of land surface temperature in relation to landscape metrics and fractional vegetation cover in an urban/peri-urban region using Landsat data

Youshui Zhang[a,b]*, Inakwu O.A. Odeh[b], and Elnazir Ramadan[c]

[a]*College of Geography, Fujian Normal University, Fuzhou 350007, China;* [b]*Faculty of Agriculture, Food and Natural Resources, The University of Sydney, Sydney, NSW 2006, Australia;* [c]*Faculty of Arts and Sciences, Qatar University, Doha 2713, Qatar*

(*Received 4 August 2011; accepted 12 April 2012*)

Land surface temperature (LST) is essentially considered to be one of the most important indicators used for assessment of the urban thermal environment. It is quite evident that land-use/land-cover (LULC) and landscape patterns have ecological implications at varying spatial scales, which in turn influence the distribution of habitat and material/energy fluxes in the landscape. This article attempts to quantitatively analyse the complex interrelationships between urban LST and LULC landscape patterns with the purpose of elucidating their relation to landscape processes. The study employed an integrated approach involving remote-sensing, geographic information system (GIS), and landscape ecology techniques on bi-temporal Landsat Thematic Mapper images of Southwestern Sydney metropolitan region and the surrounding fringe, taken at approximately the same time of the year in July 1993 and July 2006. First, the LULC categories and LST were extracted from the bi-temporal images. The LST distribution and changes and LST of the LULC categories were then quantitatively analysed using landscape metrics and LST zones. The results show that large differences in temperature existed in even a single LULC category, except for variations between different LULC categories. In each LST zone, the regressive function of LST with fractional vegetation cover (FVC) indicated a significant relationship between LST and FVC. Landscape metrics of LULC categories in each zone in relation to the other zones showed changing patterns between 1993 and 2006. This study also illustrates that a method integrating retrieval of LST and FVC from remote-sensing images combined with landscape metrics provides a novel and feasible way to describe the spatial distribution and temporal variation in urban thermal patterns and associated LULC conditions in a quantitative manner.

1. Introduction

The global urbanization rate is increasing and will continue to accelerate in the near future. It has been reported that over 45% of the world's population now live in urban areas, with over 60% projected by 2030. As the major global cities, particularly those in developing countries, continue to grow in both population and physical size, rural land-cover categories, such as soil, water, and natural vegetation, are increasingly being depleted and replaced with city impervious surfaces, such as buildings, streets, etc. These impervious surfaces have significant environmental implications, including reduction in

*Corresponding author. Email: zhangyoushui@sina.com

ISSN 0143-1161 print/ISSN 1366-5901 online

http://dx.doi.org/10.1080/01431161.2012.712227
http://www.tandfonline.com

evapotranspiration, promotion of more rapid surface runoff, increased storage and transfer of sensible heat, and reduction of air and water quality (Goward 1981; Owen, Carlson, and Gillies, 1998; Wilson et al. 2003; Chen et al. 2006). These changes, in turn, have an important impact on the local urban climate and environment, such as land surface temperature (LST), landscape aesthetics, energy efficiency, human health, and quality of life (Mcpherson et al. 1997; Xian and Crane 2006).

The assessment of urban heat condition is important for gauging the urban ecological environment. As a key surface parameter controlling most physical, chemical, and biological processes of the Earth system, LST is a consequence of surface–atmosphere interactions and energy fluxes between the land surface and Earth's atmosphere (Wan and Dozier 1996). LST is generally defined as the radiative skin temperature of the land surface (Qin and Karnieli 1999). Previous studies of measuring heat environment have been mainly based on ground observations and digital space simulation. In general, the ground observation studies provide detailed temporal variations of thermal environments, but the number of observations may be limited due to physical and economical constraints (Voogt and Oke 2003). Recent advances in remote sensing have enabled the use of satellite remote-sensing data at various spatial and temporal resolutions for estimating surface temperatures over an entire urban region (Xian and Crane 2006; Zhang et al. 2009). These advances have also enabled the estimation and inventorying of the spatial pattern of the thermal emission from the land surface over a region instantly. Hence, satellite remote sensing is increasingly growing to be a useful tool for gaining an overview of thermal variations within an urban ecosystem (Weng 2003).

Studies on LST characteristics of urban areas using satellite remote sensing have been conducted primarily using the National Oceanic and Atmospheric Administration's (NOAA's) advanced very high resolution radiometer (AVHRR) data (Owen, Carlson, and Gillies 1998; Gallo and Owen 1999; Voogt and Oke 2003; Kato and Yamaguchi 2007; Zhang, Odeh, and Han 2009). However, the 1.1 km spatial resolution of AVHRR data is suitable only for mapping temperature at the continental or global scale. As Moderate Resolution Imaging Spectroradiometer (MODIS) and Advanced Spaceborne Thermal Emission and Reflection Radiometer (ASTER) data have become readily available in recent years, the multiple thermal infrared (TIR) bands of these sensors provide better results for LST studies at various spatial scales (Kato and Yamaguchi 2007) than AVHRR data. Moreover, both MODIS and ASTER data have multiple bands in visible and near-infrared (VNIR), shortwave infrared (SWIR), and TIR wavelengths, although the MODIS spatial resolution varies, i.e. 250 m for bands 1 and 2, 500 m for bands 3–7, and 1000 m for bands 8–36. MODIS data, therefore, would be more suitable for continental and global scale studies related to Earth's surface thermal features than for local scales. ASTER data, with spatial resolutions varying from 15 m for the visible bands to 30 m for the near-infrared bands and 90 m for the TIR bands, thus provide much more detailed information than MODIS, and are more suitable for urban-related studies at local scales than either AVHRR or MODIS data. However, for a regional study, ASTER products are too expensive for such a large coverage. The alternatives are the Landsat Thematic Mapper (Landsat-TM or Enhanced Thematic Mapper Plus (ETM+)) products characterized by 30 m spatial resolution for bands 1–5 and 7, and 120 m (TM) or 60 m (ETM+) band 6, which are now available at no cost from NASA. Although images produced by the Landsat-TM sensors (Wilson 1988) are generally too coarse for identification of individual structures, they are sufficient to detect significant spatial and temporal variations in urban vegetation and surface temperature (Woodcock and Strahler 1987).

A related feature that is closely linked to LST is the fractional vegetation cover (FVC). It is one of the most important variables in land surface modelling that provides a

continuous field to complement discrete land-cover classification. As an important parameter in the physics of land surface processes at regional and global scales, vegetation is an important component of the urban ecosystem, influencing urban thermal characteristics that have been the subject of much basic and applied research in recent years (Gallo et al. 1993; Carlson, Gillies, and Perry 1994; Nichol 1996; Gillies et al. 1997; Owen, Carlson, and Gillies 1998). Urban vegetation influences the physical environment of cities through selective absorption and reflection of incident radiation and regulation of latent and sensible heat exchange (Carlson, Gillies, and Perry 1994; Gillies et al. 1997). The abundance of urban vegetation, through its spatial distribution, also influences air quality and human health. Urban forests provide shadows and block winds that help to maintain relatively low LSTs in urban areas, which may lead to lower fuel usage (Liu and Weng 2008). Remote sensing is a useful tool for studying and quantifying the extent and the change of urban vegetation. Thus, by integrating remote-sensing and geographic information system (GIS) techniques, we can apply FVC to study the relationship between landscape patterns and LST.

A combination of vegetation cover and LST provides a powerful parameter for describing the characteristics of landscape patterns and processes. To understand the dynamics and processes and their interactions of a heterogeneous land cover such as an urban landscape, one must be able to accurately quantify its spatial pattern and temporal changes (Wu et al. 2000). Landscape or land-use/land-cover (LULC) patches in a region may have different sizes, shapes, and spatial arrangements, the consequence of spatial heterogeneities of the landscape (Liu and Weng 2008, 2009). It is known that LULC categories have significant effects on many ecological processes (Pan et al. 2001; Bain and Brush 2004; Bender et al. 2005) and are linked to distinct behaviours of the urban thermal environment (Voogt and Oke 1997; Weng, Lu, and Schubring 2004). Therefore, to understand the landscape dynamics and processes, one must be able to accurately quantify the spatial pattern and its temporal changes (Wu et al. 2000). A series of landscape metrics have been developed to characterize the spatial patterns of landscapes, to study the ecological quality, and to elucidate the influence of LULC patterns on the environment (O'Neill, Krummel, and Gardner 1988; Riitters, O'Neill, and Hunsaker 1995; Gustafson 1998; Yue et al. 2007; Liu and Weng 2008). However, landscape metrics are not commonly used to analyse the relationship between LULC and LST.

Landsat imagery has an appropriate spatial resolution for the spatial scale of the study area. The methodology employed Landsat-TM data to explore landscape patterns in relation to urban thermal characteristics. Specifically, the study aimed at (1) examining the relationship between landscape (LULC) patterns and thermal properties at the regional scale as characterized by landscape metrics and (2) exploring the landscape composition and the structure of each LST zone to understand the relationship between LULC and LST. To achieve these aims, two bi-temporal Landsat-TM images covering much of metropolitan Sydney and its fringe area – acquired at approximately the same season in 1993 and 2006 – were used as a case study. LST, LULC, FVC, and landscape metrics were derived from the images to quantify the spatial characteristics of the landscape (LULC) pattern and associated surface thermal spatial distribution and variability over time.

2. Data and methods

2.1. The study region

The study region is southwestern metropolitan Sydney and its fringe area (Figure 1). Sydney is Australia's largest city and is located on the east coast of the continent, at approximate latitude 34° 00′ S and longitude 151° 00′ E. According to the 2008 estimate, Sydney

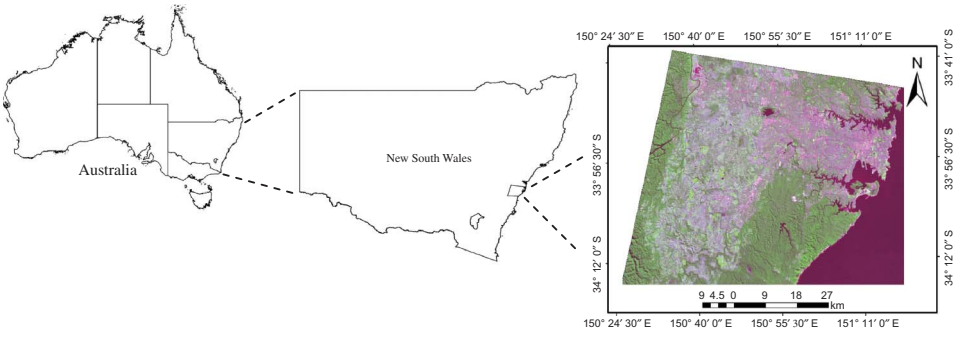

Figure 1. Geographical location of the study area.

had a population of approximately 4.34 million, and attained this level from a population of 3.5 million in 2003 (Smith 2003). The study area is approximately 3310 km^2. Climatically, Sydney is temperate and is characterized by warm summers and cool winters. The warmest month is January, with an average air temperature range of 18.6–25.8°C. There are, on average, 14.6 days in a year with air temperatures over 30°C. The winter is mildly cool; the coldest month is July, with an average range of 8–16.2°C. Rainfall is spread fairly evenly throughout the year, and the average annual rainfall, with moderate to low variability, is 1217 mm.

In recent years, Sydney has experienced a fast population growth, which invariably has led to urban expansion (Smith 2003; ABS 2003). This expansion is noticeable in the western and southwestern parts of the city, where accelerated development has been taking place since the early 1990s. The urban sprawl of Sydney occurs through encroachment into the adjacent agricultural and peri-urban areas, which has caused large-scale land-use/land-cover change (LUCC), leading to perturbation of the ecosystems.

2.2. Image acquisition and land-use/land-cover mapping

Bi-temporal Landsat-TM images (path 89/row 84) acquired on 25 July 1993 and 29 July 2006, respectively, were the primary data for deriving LST and LULC types. Because the urban vegetation in Sydney in the winter months is green, the bi-temporal images taken in middle of winter (July) were considered ideal for research on LST spatial distribution with LULC and FVC and their changes. The two images (downloaded from the website http://glovis.usgs.gov/) were processed at Level 1T by incorporating ground control points, while also employing a digital elevation model (DEM) for topographic accuracy, leading to systematic radiometric and geometric accuracy (http://edcsns17.cr.usgs.gov/helpdocs/landsat/product_descriptions.html#terrain_l5_l1t). The images were rectified and projected to the universal transverse mercator (UTM) system (spheroid World Geodetic System (WGS) 84, datum WGS 84, and zone 56). Further processing using a DEM for topographic accuracy was also carried out in the Landsat terrain-corrected product Level 1T. Each of the Landsat-TM images consists of seven spectral bands: bands 1–5 and band 7 with spatial resolution of 30 m, and TIR band 6, which is resampled from its original resolution of 120 m onto 60 m using a cubical convolution algorithm.

The original pixel values of the two images were converted to exo-atmospheric reflectance based on the methods of Chander and Markham (2003). Later, the atmospheric correction was done by Second Simulation of the Satellite Signal in the Solar Spectrum

(6S) radiative transfer code, the outputs of bands 1–5 and band 7 take the unit of proportional reflectance, ranging from 0 to 1. In order to analyse LULC patterns and LST on a common spatial resolution, bands 1–5 and band 7 of two-temporal images were resampled into 60 m using the cubical convolution algorithm. In addition, a rectified and projected 2000 IKONOS image of the Sydney region with a spatial resolution of 4 m was used as a reference for the recognition and classification of LULC categories using the Landsat images.

To produce LULC maps, we applied a supervised maximum-likelihood classifier using all but band 6 in each case. Based on our preliminary analysis of the expected urban and rural LULC categories in the study region, we used a modified Level II of the Australian Collaborative Land-Use Mapping Program (ACLUMP) (BRS 2006). Therefore, five LULC categories were identified: (1) urban, (2) water (excluding the sea), (3) grassland, (4) forest, and (5) agriculture. Random sampling was adopted for the accuracy assessment, the reference LULC categories were based on visual interpretation of TM and IKONOS imagery, and the overall classification accuracy in both cases was above 80%. It should be noted that the purpose here was not to compare the accuracy using different images, but rather to produce consistent LULC maps in order to provide an insight into the relationships between landscape patterns and the changing urban thermal environment. This would lead to a better understanding of the environmental influence of LULC change on the urban ecosystems.

2.3. Derivation of LST and delineation of LST zones

The derivation of LST from the Landsat-TM thermal data requires several procedures: sensor radiometric calibrations, atmospheric and surface emissivity corrections, and characterization of spatial variability in land cover, among other procedures. As described above, the Landsat-TM TIR (band 6) data were used to derive the LST. The study applied the method for deriving LST in three steps as proposed by Yuan and Bauer (2007). In step 1, the digital numbers (DNs) of band 6 were converted to radiation luminance or top-of-atmosphere (TOA) radiance (L_λ) using the following formula (Chander and Markham 2003):

$$L_\lambda = \frac{(L_{\max} - L_{\min})}{(\mathrm{QCAL}_{\max} - \mathrm{QCAL}_{\min})}(\mathrm{DN} - \mathrm{QCAL}_{\min}) + L_{\min}, \quad (1)$$

where λ is TIR band 6; L_λ is the TOA radiance at the sensor's aperture in W m^{-2} sr^{-1} μm^{-1}; $\mathrm{QCAL}_{\min} = 0$, the lowest value in the range of rescaled radiance in DN; $\mathrm{QCAL}_{\max} = 255$, the highest value in the range of rescaled radiance in DN; $L_{\min}$ is the TOA radiances for band 6 at DNs $\mathrm{QCAL}_{\min}$ in W m^{-2} sr^{-1} μm^{-1}; and $L_{\max}$ is the TOA radiances for band 6 at DNs $\mathrm{QCAL}_{\max}$ in W m^{-2} sr^{-1} μm^{-1}. $\mathrm{QCAL}_{\min}$, $\mathrm{QCAL}_{\max}$, $L_{\min}$, and $L_{\max}$ are given in the header file of the images.

Step 2 involves the conversion of TOA radiance to surface-leaving radiance by removing the effects of the atmosphere in the thermal region. An atmospheric correction tool – Moderate-Resolution Atmospheric Transmission (MODTRAN)-4.0 for the thermal band of Landsat sensors – was used in this study. This tool involves the MODTRAN radiative transfer code and a suite of integration algorithms to estimate three parameters – atmospheric transmission, upwelling radiance, and downwelling radiance – which allows surface-leaving radiance L_T or the radiance of a blackbody target of kinetic temperature T to be calculated using Equation (2):

$$L_T = \frac{L_\lambda - L_\mu - \tau\,(1-\varepsilon)\,L_d}{\tau\varepsilon}, \tag{2}$$

where L_T is the radiance of a blackbody target of kinetic temperature T; L_μ is the upwelling or atmospheric path radiance; L_d is the downwelling or sky radiance; τ is the atmospheric transmission, and ε is the emissivity of the surface specific to the target type.

Radiance values are in units of W m^{-2} sr^{-1} μm^{-1} and the transmission and emissivity are unitless. The emissivities are based on the land-cover classification and the emissivity values as derived by Snyder et al. (1998).

In the final step, the radiance (L_T) is converted to surface temperature using the Landsat specific estimate of the Planck curve (Equation (3); Chander and Markham (2003)):

$$T = \frac{K_2}{\ln\left[\left(K_1/L_T\right) + 1\right]}, \tag{3}$$

where T is the temperature in kelvin (K), K_1 is the pre-launch calibration constant in W m^{-2} sr^{-1} μm^{-1}, and K_2 is another pre-launch calibration constant in kelvin. For Landsat 5 TM, $K_1 = 607.76$ W m^{-2} sr^{-1} μm^{-1} and $K_2 = 1260.56$ K.

As atmospheric water vapour content varies over time due to seasonality and inter-annual variability of the atmospheric conditions, it is not appropriate to directly compare the surface temperature or LST of different seasons or years. In order to circumvent this, we subdivided the LST values into four different zones based on multiples of standard deviation (SD) by adding or subtracting the standard deviation of LST from its mean, which was inspired by the methods used in data classification by Smith (1986) and Liu and Weng (2008). The four zones were therefore created using the following LST intervals:

$$\begin{aligned}
&\text{Zone 1} = \text{LST} \leq (\text{Mean}_{\text{LST}} - 2\,\text{SD}),\\
&\text{Zone 2} = \text{LST} > (\text{Mean}_{\text{LST}} - 2\,\text{SD}) \cup \text{LST} \leq \text{Mean}_{\text{LST}},\\
&\text{Zone 3} = \text{LST} > \text{Mean}_{\text{LST}} \cup \text{LST} \leq (\text{Mean}_{\text{LST}} + 2\,\text{SD}),\\
&\text{Zone 4} = \text{LST} > (\text{Mean}_{\text{LST}} + 2\,\text{SD}).
\end{aligned} \tag{4}$$

The LST intervals for the statistical zones are shown in Table 1. These statistical zones are suited for comparison between the two periods and therefore can be used to quantitatively analyse the spatial distribution and relationships of FVC, landscape metrics, and LST based on each LST zone.

Table 1. Means, standard deviations (SD), and interval values used to create the LST zones.

Image acquisition date	Mean LST	SD	Zone 1	Zone 2	Zone 3	Zone 4
25 July 1993	282.80	1.00	<280.80	280.80–282.80	282.80–284.80	>284.80
29 July 2006	285.60	1.31	<282.98	282.98–285.60	285.60–288.22	>288.22

2.4. Derivation of FVC

FVC, the ratio of vegetation occupying a unit area, is a significant parameter in the development of climate and ecological models. It is indispensable information of many global and regional climate numerical models. FVC depicts the amount and nature of vegetation cover, and modulates the proportions of vegetation and ground (e.g. bare soil) visible to a sensor (Sandholt, Rasmussen, and Andersen 2002). The difference between the radiative temperature of the vegetation canopy and that of the ground affects the magnitude of LST. The FVC of each pixel was obtained by a spectral mixture analysis technique. In this study, we used the simple and effective normalized difference vegetation index (NDVI) to estimate FVC based on the following expression (Wittich and Hansing 1995):

$$\mathrm{NDVI}_i = f_c \times \mathrm{NDVI}_v + (1 - f_c) \times \mathrm{NDVI}_s, \tag{5}$$

which can be rewritten as follows:

$$f_c = \frac{\mathrm{NDVI}_i - \mathrm{NDVI}_s}{\mathrm{NDVI}_v - \mathrm{NDVI}_s}, \tag{6}$$

where NDVI_i is NDVI value of a pixel i; f_c is FVC ranging from 0 to 1; NDVI_v is the value for a pure green vegetation pixel; and NDVI_s is the value for a bare soil pixel.

FVC has been used to study changes in vegetation cover using images for different dates (Price 1987; Che and Price 1992; Carlson and Arthur 2000).

2.5. Computation of landscape metrics

The need to quantify the spatial heterogeneity of the landscape is to elucidate the relationships between landscape processes and spatial landscape patterns (Turner 1990; Turner et al. 2003). Therefore, the measurement, analysis, and interpretation of spatial landscape patterns have received much attention in landscape ecology (Haines, Young, and Chopping 1996). Landscape metrics are used to quantify landscape composition and configuration on maps or remotely sensed images. Many of the applications focus on ecological analysis (e.g. Frohn and Hao 2006). In the case of application on LULC analysis, the number of LULC categories, their proportions, and spatial structure evidently affect LST (Weng et al. 2004; Liu and Weng 2008). In this study, four selected landscape metrics were used to quantitatively analyse the relationship between the metrics derived from LULC and LST. The metrics were derived using the computer program FRAGSTATS (McGarigal et al. 2002).

Patch density (PD) is a useful metric of landscape configuration. Computation of the number of patches per unit area of a specific LULC category is a good way to measure the spatial heterogeneity of a given landscape, which facilitates comparisons among LULC categories of varying sizes. PD for a particular LULC category could serve as a good index of fragmentation. The density of a given LULC type for the entire landscape can be derived as follows:

$$\mathrm{PD} = \frac{N \times 10^6}{A}, \tag{7}$$

where N is the total number of patches in the landscape and A is the total landscape area (m^2).

As stated above, PD is expressed as a unit per 100 ha, which serves as a good index of heterogeneity, and thus facilitates comparisons among landscapes of varying sizes.

In landscape ecology, the perimeter–area fractal dimension index (PAFRAC) is used to measure the shape complexity of patch types. In applying it to LULC analysis, as was the case here, it provides a measure of human impact on the landscape. This is based on the assumption that natural boundaries have complex shapes, and that as human disturbance increases, the PAFRAC decreases, approaching 1. Since the edges of one patch are also edges of adjacent patches, the edge/area ratios also provide information about the overall shape complexity of the landscape. Thus, the PAFRAC represents shape complexity (a departure from Euclidean geometry), which has been effectively used to represent human-induced disturbance. PAFRAC can be derived as follows:

$$\mathrm{PAFRAC} = \frac{2}{\left[N\sum_{i=1}^{m}\sum_{j=1}^{n}\left(\ln p_{ij}\ln a_{ij}\right) - \left(\sum_{i=1}^{m}\sum_{j=1}^{n}\ln p_{ij}\right)\left(\sum_{i=1}^{m}\sum_{j=1}^{n}\ln a_{ij}\right)\right] \Big/ \left[\left(N\sum_{i=1}^{m}\sum_{j=1}^{n}\ln^2_{p_{ij}}\right) - \left(\sum_{i=1}^{m}\sum_{j=1}^{n}\ln p_{ij}\right)^2\right]}, \tag{8}$$

where a_{ij} is the area of patch ij, p_{ij} is the perimeter of patch ij, and N is the total number of patches in the landscape.

Another metric that could be useful for studying land-cover patterns is the aggregation index (AI); it identifies the tendency of the spatial aggregations for specific patch types. AI is calculated from an adjacency matrix of pixels, which is indicative of the frequency with which different pairs of patch types (including adjacencies between the same patch types) appear side-by-side in the landscape (McGarigal et al. 2002):

$$\mathrm{AI} = \frac{g_{ij}}{\max\left(g_{ij}\right) \times 100}, \tag{9}$$

where g_{ij} is the number of like adjacencies (joins) between pixels of patch type (class) i based on the single-count method and $\max(g_{ij})$ is the maximum number of like adjacencies (joins) between pixels of patch type (class) i based on the single-count method.

The AI metric provides a quantitative basis to correlate spatial patterns with processes that are typically class-specific (He, DeZonia, and Mladenoff 2000).

The last but not least of the metrics used here is the mean patch size (MPS), which represents the average area of all patches of the corresponding LULC types in the landscape. It can be computed as follows:

$$\mathrm{MPS} = \frac{\sum_{i=1}^{N} A_i}{N}, \tag{10}$$

where A_i is area of patch i of a given LULC and N is the total number of patches of a given LULC.

These four landscape metrics can provide the quantitative link between landscape patterns and ecological or environmental processes. They are derived at three levels: patch level, class level, and landscape level (McGarigal et al. 2002). In this study, the selected metrics were analysed at the class level, integrated for all of the patches of a given metric.

These metrics were then applied to elucidate the spatial landscape patterns within the different LST zones. The landscape metric value is directly dependent on the resolution and extent (scale) of the data and the classification scheme used to define landscape cover types from remote-sensing images (Turner, Gardner, and O'Neill 2001). To minimize the effects of these limitations, we consistently used images of the same spatial resolution (60 m) and spatial extent.

3. Results

3.1. LULC change between the two dates

The spatial patterns of the LULC categories resulting from classification are presented in Figure 2. Even though classification accuracy was not the main focus of this study, it is worth noting that the overall classification accuracy of the two maps was above 85%. On both dates, water LULC patches, the smallest in terms of areal proportion, were fairly distributed throughout the study region. In contrast, although urban LULC category was predominant in the northern part of the study region, grassland was mainly mosaicked within urban and agricultural land uses. To complete the picture, forest was confined mainly to the south of the study region with agriculture mainly distributed in the west and southwest of the study region.

Comparison of the two LULC maps for the two dates indicated a remarkable urbanization increase in the region, which is not surprising. Table 2 shows the proportion of the LULC categories for the two dates, with urban area increasing from 21.21% of the total area in 1993 to 27.98% in 2006. Agriculture increased slightly from less than 22.35% in 1993 to 25.46% in 2006. In contrast, the proportion of grassland in 2006 was less than half the proportion of 1993, i.e. declining from 14.08% in 1993 down to 6.95% in 2006. While the water LULC category had the lowest areal proportion, forest had the largest areal proportions in both years. However, the two LULC categories did not show any significant change in proportions between the two dates. Further analysis of LULC indicated where LULC changes had occurred (Table 2). The swap changes occurred mainly in the southwest and west of the study area, which had experienced the most rapid urban expansion and where grassland was being replaced by agriculture since the early 1990s. However, it is worth mentioning that LULC change is not the focus of this study.

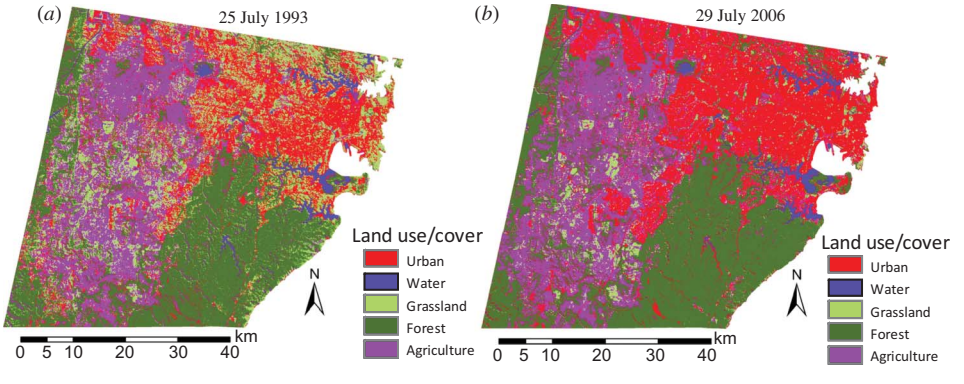

Figure 2. Spatial patterns of LULC types of the study area in two periods.

Table 2. Land use/cover change (LUCC) in 1993 and 2006.

	Urban		Water		Grassland		Forest		Agriculture	
Date	Area (km^2)	%	Area (km^2)	%	Area (km^2)	%	Area (km^2)	%	Area (km^2)	%
1993	702.051	21.21	124.787	3.77	466.048	14.08	1277.329	38.59	739.785	22.35
2006	926.138	27.98	83.743	2.53	230.045	6.95	1227.348	37.08	842.726	25.46
Changes	−224.09	−6.77	41.05	1.24	236.01	7.13	49.98	1.51	−102.95	−3.11

3.2. *LST patterns and variations within each LULC category*

The spatial distribution patterns of LST, which is indicative of the relative magnitude of surface temperature, are shown in Figure 3. Statistically, the bi-temporal LST derived for the two dates had a mean value of 282.8 K in 25 July 1993 and 285.60 K in 29 July 2006. The range of LST values is 273 K–289 K for 1993 and 273 K–293 K in the case of 2006. On both dates, the estimated highest surface temperature mainly existed in the urban areas (including the central business district, industrial districts, airport, and high-density residential areas) and in the unplanted agriculture fields of rural areas. The cooler areas were mainly associated with forests, grass, and agricultural fields with actively growing crops. The lowest temperature values were estimated for the southern and western forest LULC. Also on both dates, the estimated water temperature values were close to the overall mean LST. It is well known that the LST is characterized by seasonal variation, and that agricultural activities are influential on the interpretation of LULC effects on LST (Vinnikov *et al*. 2008).

To explicate the LST patterns and variation within the different LULC categories, the basic statistics (mean LST and its standard deviation) of each category were estimated by averaging all corresponding pixel values. The mean LST of urban was 282.56 K on 25 July 1993, whereas the urban mean LST was slightly higher at 286.05 K on 29 July 2006 (Table 3). However, the mean LST values for the non-urban LULC categories were

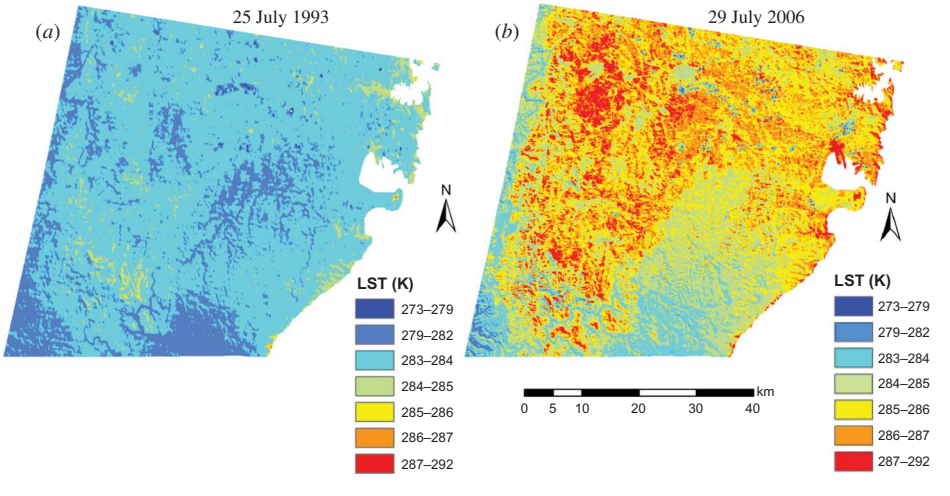

Figure 3. Land surface temperature of the study region in (*a*) 1993 and (*b*) 2006.

Table 3. Mean and standard deviation (SD) of LST in each LULC category for the two dates.

	Urban		Water		Grassland		Forest		Agriculture	
Date	Mean LST (K)	SD	Mean LST (K)	SD	Mean LST (K)	SD	Mean LST (K)	SD	Mean LST (K)	SD
1993	282.56	1.08	282.45 (0.11)	1.30	283.37 (–0.81)	0.83	282.36 (0.20)	0.85	283.26 (–0.70)	0.85
2006	286.05	1.27	285.47 (0.58)	1.18	286.28 (–0.23)	0.92	284.69 (1.36)	1.04	286.31 (–0.26)	1.01

Note: The LST differences between urban and other LULC categories are in parentheses.

slightly higher for grassland and agriculture and slightly lower for water and forest when compared with the mean urban LST. It is interesting to note that in 2006, forest experienced by far the largest difference in LST (−1.36 K) from that of urban, but much less so in 1993 (Figure 3). The physical basis for grassland and agriculture experiencing higher LST than urban is covered in Section 4.

The results of zone creation are shown in Figure 4. It is evident that there were some instances where significant zonal changes had occurred between the two dates, particularly the zones associated with urban, grassland, and agriculture categories (Table 4). The magnitude of differences in zonal areas between the two dates among the zones associated with urban are more pronounced in zone 1, with urban LULC increasing more than 30-fold between 1993 and 2006, followed by zone 2 (increased by 10 times between 1993 and 2006). The difference for zone 3 is insignificant. However, in zone 4, the difference is the reverse, with the decline of urban LULC coverage by over 80 times. One reason for the differences is urban expansion, which had increased by nearly one-third between 1993 and 2006 (Table 2). Another possible explanation may be ascribed to variations of the urban LULC categories, characterized by juxtaposed concrete and hard surfaces interspersed with spotty patches of vegetation (consisting of urban forest or parklands and recreational areas covered by grassland). The latter may have been exaggerated by the differences in the prevailing weather conditions at the time of satellite image acquisition. For this same reason, grassland experienced decline in area in all of the zones between the two dates. However, forest showed an obvious increase between 1993 and 2006 in zones 2 and 3. Note that the

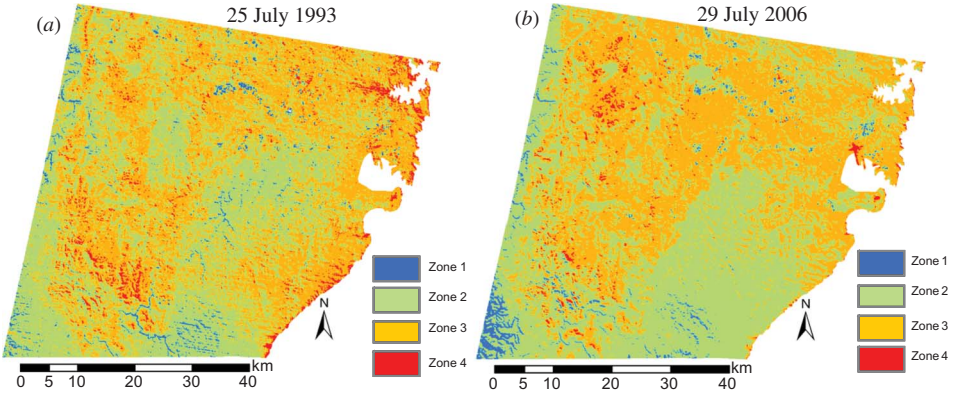

Figure 4. Land surface temperature zones in (*a*) 1993 and (*b*) 2006.

Table 4. Proportion of LULC categories (areal and %) in each LST zone for the two dates.

	Zone 1				Zone 2				Zone 3				Zone 4			
	1993		2006		1993		2006		1993		2006		1993		2006	
	Area (km^2)	%	Area (km^2)	%	Area (km^2)	%	Area (km^2)	%	Area (km^2)	%	Area (km^2)	%	Area (km^2)	%	Area (km^2)	%
Urban	0.662	0.02	21.515	0.65	20.522	0.62	231.369	6.99	362.114	10.94	669.613	20.23	318.753	9.63	3.641	0.11
Water	10.592	0.32	3.310	0.10	52.298	1.58	43.361	1.31	54.946	1.66	36.410	1.10	6.951	0.21	0.662	0.02
Grassland	0.662	0.02	0.331	0.01	88.377	2.67	59.249	1.79	347.881	10.51	164.838	4.98	29.128	0.88	5.627	0.17
Forest	31.114	0.94	48.657	1.47	788.773	23.83	995.317	30.07	448.505	13.55	183.374	5.54	8.937	0.27	0.033	<0.01
Agriculture	2.648	0.08	0.993	0.03	220.115	6.65	230.045	6.95	486.570	14.70	596.793	18.03	30.452	0.92	14.895	0.45
Total	45.678	1.38	74.806	2.26	1170.085	35.35	1559.341	47.11	1700.016	51.36	1651.028	49.88	394.221	11.91	24.858	0.75

distribution pattern of forest in urbanized areas was in scattered spotty patterns in 1993, but less so in 2006, which was probably due to some limited urban replacement of forest patches in urban zones between 1993 and 2006 (Figure 2). During the same time span, the proportion of water declined in all of the four zones (Table 4). In addition, it appears that agriculture declined in zones 1 and 4, but increased in zones 2 and 3 between 1993 and 2006. As pointed out, this is because of a combination of seasonal climatic effect on the LST as it was used for zoning and also because of swapping of LULC categories, e.g. urban replacing grassland, agriculture swapping for grassland, and disappearance of some of the within-urban forest areas due to urban development.

To identify the impact of each LULC on LST, the binary maps of individual LULC category were created from Figure 2 and then overlain on the LST zonal maps (Figure 4) to obtain zonal statistics (mean and standard deviation) of each LST zone. Table 5 shows the summary of the two statistics for the two dates. As would be expected, urban zone 4 exhibited the largest LST for both dates, and with the exception of zone 1, it has the highest dispersion as estimated by the standard deviation. In urban zone 1 for both dates however, the mean LST was mainly lower than the mean for any other LULC categories. In comparing all of the LST zones other than those of water, it can be observed that the zonal LST standard deviations of urban areas were generally higher than those of the other LULC categories, with only a few exceptions (grassland zone 3 on both dates). This is particularly the case for urban zone 1. This is suggestive of the fact that the urban vegetation is spotty with spotty sizes mostly less than the working 60 m resolution of the original images used for the study. Moreover, the pixels of urban areas, in many instances, probably consisted of a mixture of grassland (mainly grass lawns) and patchy forest interspersed with impervious surfaces that generally characterize urban land cover. In general, both zones 1 and 4 of urban have larger standard deviations than those of urban middle zones (zones 2 and 3), indicating that the pixels of the middle zones are more homogeneous than the lower or higher zones.

The zonal LST statistics in Table 5 also show that water, grassland, and forest had nearly the same trend in mean zonal LST and standard deviation, with the latter higher for

Table 5. Summary statistics of LST zones for LULC categories determined for the two dates.

Date	LST zone	Mean LST and SD	Urban	Water	Grassland	Forest	Agriculture
25 July 1993	Zone 1	Mean (K)	279.03	280.15	280.44	280.28	279.89
		SD	1.60	0.38	0.00	0.28	0.79
	Zone 2	Mean(K)	282.04	281.81	282.20	281.96	282.15
		SD	0.43	0.53	0.34	0.45	0.35
	Zone 3	Mean (K)	283.22	283.48	283.49	283.25	283.40
		SD	0.48	0.52	0.49	0.43	0.48
	Zone 4	Mean (K)	285.58	284.96	285.02	284.94	285.01
		SD	0.68	0.25	0.36	0.23	0.34
29 July 2006	Zone 1	Mean (K)	280.96	281.94	282.60	282.30	281.75
		SD	1.83	0.73	0.00	0.46	1.23
	Zone 2	Mean (K)	284.96	284.96	285.12	284.50	285.07
		SD	0.65	0.64	0.50	0.74	0.55
	Zone 3	Mean (K)	286.49	286.32	286.60	286.21	286.67
		SD	0.54	0.45	0.56	0.37	0.58
	Zone 4	Mean (K)	289.21	288.46	288.58	288.30	288.50
		SD	0.67	0.28	0.46	0.00	0.34

Note: SD, standard deviation.

the middle zones 2 and 3 than for zones 1 and 4. This is in contrast to the trend for the urban zonal LST dispersion described above. It is also indicative of the fact that the more homogeneous of these LULC types exhibit more uniform lower LST standard deviation than the case otherwise. Water in the eastern area, comprising mainly rivers and dams, had higher surface temperature than the western lakes because of the maritime influence on the former. Forest in zone 4 was usually located in sunny slope and in zone 1 was usually in shady slope. Like urban in zone 1, agriculture in zone 1 had the lowest LST with the highest standard deviation; the reason being that the agriculture pixels in zone 1 were a mixture of the actively growing crops and unplanted bare soil. For the same reason, agriculture in zone 4 was characterized by the highest LST and had the lowest standard deviation, which is probably due to the fact that these areas consisted of mainly unplanted bare soil, as bare surfaces are usually characterized by higher LST than planted crop covers. Thus, the trend of agriculture is that it shifts from actively growing crops in zone 1, decreasing in vegetation coverage, to bare soil areas in zone 4. Based on this trend, we can explain agriculture activities and analyse its impact on the thermal environment at any given time in the season or year.

Generally, the 2006 LST and standard deviation values of LULC categories in each LST zone were higher than those in 1993. The main reason is probably due to differences in the prevailing weather conditions at the time of image acquisition and the change in LULC between the two dates. Thus, the detailed analysis of LULC categories in relation to the LST zones provides useful information about the urban thermal environment and how different LULC categories affect the thermal signatures. This means that it is possible to alleviate the urban heat island (UHI) effect by optimizing land-use planning based on this type of information. It is well known that LULC change would influence the UHI distributions, but proper land-use planning could alleviate temperature rise, for example by allocating positive contributive LULC categories (Liu and Weng 2008).

3.3. Relationship between LST and FVC

As important basic data for describing ecosystems, FVC is also a key parameter in thermal remote-sensing analysis from which surface emissivity can be estimated (Quattrochi and Ridd 1998; Zhang, Odeh, and Han 2009). For an area characterized by partial vegetation cover, surface thermal properties have a great influence on LST through the thermal processes of conduction, convection, and radiation. Therefore, thermal responses by vegetation cover can be highly varied as a function of the biophysical properties of the vegetation itself (Quattrochi and Ridd 1998; Pena 2008). In addition, as explained in Section 3.1, because the planted and fallow agricultural areas are characterized by difference in LST patterns, FVC could be a useful tool for analysing agricultural activities.

Figure 5 shows the FVC of the study area on both dates. It is clear from the FVC patterns in comparison to Figure 2 that vegetation LULC categories (grassland and forest), which should have high FVC close to 100%, are less abundant in urban areas, and that considerable urban expansion had occurred in the 13 years period.

In order to improve understanding the variance of FVC and LST in different LULC categories, the pixel values of FVC and LST are derived based on the west–east profiles (Figure 6). The west–east profiles start with forest; through agriculture (planted and unplanted areas); urban area (road, built-up area including industrial, commercial and residential areas, and so on) with forest, water (lake), and grassland (park); and end at airport of urban area. For FVC profiles, values in built-up, water, and unplanted areas are far lower

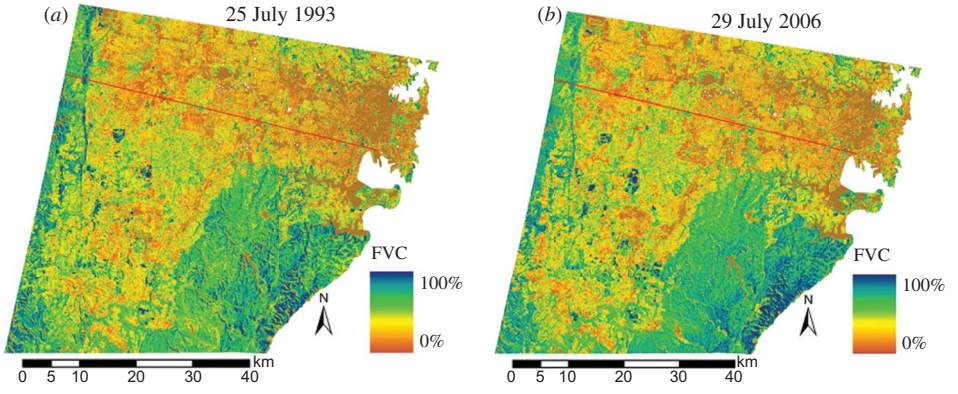

Figure 5. Spatial distribution of fractional vegetation cover derived from the bi-temporal images acquired in (*a*) 1993 and (*b*) 2006 (red lines represent west–east profiles of FVC and LST across the research area).

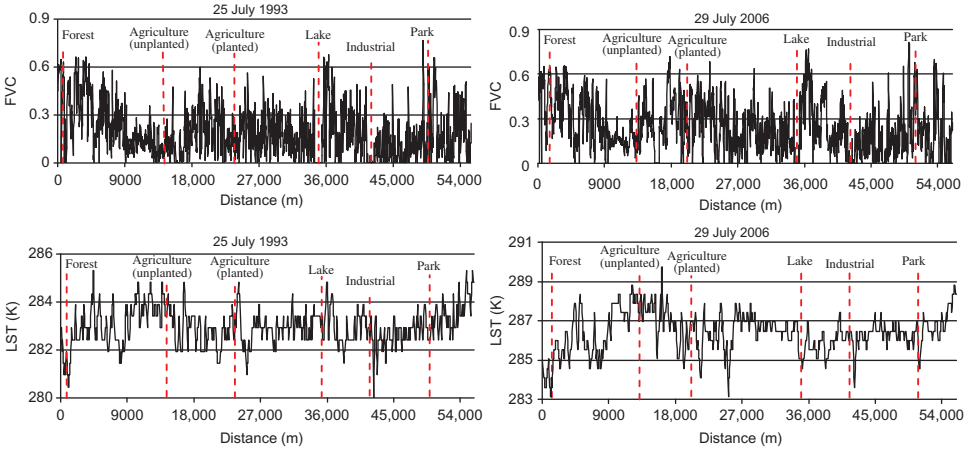

Figure 6. FVC and LST variance along the west–east profiles in Figure 5.

than other areas. As for LST profiles, the effect of the urban thermal environment is obvious from suburb to urban, LST values are relatively higher in urban area and unplanted agriculture areas than other areas. Figure 6 shows that the peaks of FVC appear at forest and grassland (park). The peaks of LST are usually the areas where unplanted agriculture and urban built-up areas are located, whereas the troughs are areas where water, grassland, and forest are found. FVC had a reverse trend with LST, except for water, and their change trends are closely related to the urban sprawl and impacted by agriculture activities.

In Figure 6, FVC has an inverse relationship with LST. In support of this notion and by comparing Figures 3 and 5, we derived the mean zonal FVC shown in Table 6. Clearly, there is a decrease in %FVC as the zone number increases, meaning higher LST, which illustrates a clear relationship of %FVC with LST, as the latter was used for the creation of the zones.

Table 6. Mean zonal FVC as derived for each LST zone.

	Zonal mean FVC (%)			
Date	Zone 1	Zone 2	Zone 3	Zone 4
25 July 1993	0.35	0.34	0.31	0.30
29 July 2006	0.45	0.45	0.27	0.25

In order to elucidate the relationship of LST with %FVC, a number of zonal regression functions were fitted, with LST as a dependent variable and FVC as an independent variable. Table 7 shows the regression functions for the two dates and all LULC categories, except the water LULC type. With the exception of a few cases for zone 1, Pearson's correlation coefficients (r) show a significant but moderate to high inverse linear relationship of LST with FVC. For most of the latter cases, while FVC decreased, LST increased. In zone 1, NDVI usually has saturation values, FVC values are high, and the correlation coefficients between LST and FVC are comparatively low. Zone 4 is the high-density urban and unplanted agricultural areas, and the correlations are also not obvious here. The results indicate that FVC is an indicator of LST with a linear relationship, especially in LST zones

Table 7. Linear regression of LST as a function of FVC for each LST zone versus LULC for the two dates.

		Regression equation			
Image	LULC category	Zone 1	Zone 2	Zone 3	Zone 4
1993	Urban	$y = 279.02+2.42x$ N: 269 r: 0.47 SD:1.023	$y = 282.27–0.70x$ N:258 r: –0.43 SD: 0.367	$y = 283.27–0.47x$ N:117 r: –0.63 SE: 0.381	No data
	Grassland	$y = 280.27+0.86x$ N: 66 r: 0.53 SE: 0.22	$y = 282.24–0.13x$ N:217 r: –0.66 SE: 0.316	$y = 283.83–0.13x$ N:2147 r: –0.54 SE: 0.459	$y = 285.12–0.20x$ N:756 r: –0.67 SE: 0.280
	Forest	$y = 280.08+0.285x$ N: 1228 r: 0.30 SE: 0.343	$y = 281.97–0.21x$ N:2009 r: –0.46 SE: 0.36	$y = 283.26–0.357x$ N:692 r: –0.51 SE: 0.406	$y = 284.80–0.23x$ N:132 r: –0.49 SE: 0.192
	Agriculture	$y = 279.9–1.69x$ N: 24 r: –0.51 SE: 0.85	$y = 281.93–1.44x$ N:38 r: –0.64 SE: 0.365	$y = 283.29–0.9x$ N:295 r: –0.73 SE: 0.459	$y = 285.03–0.62x$ N:671 r: –0.42 SE: 0.345
2006	Urban	$y = 281.347+1.28x$ N: 135 r: 0.403 SE: 1.160	$y = 284.79–0.03x$ N:108 r: –0.51 SE: 0.56	$y = 286.63–0.48x$ N:2496 r: –0.78 SE: 0.433	$y = 288.08–2.41x$ N:77 r: –0.65 SE: 0.372
	Grassland	$y = 279.70+4.48x$ N: 18 r: 0.65 SE: 0.912	$y = 285.30–0.08x$ N:585 r: –0.74 SE: 0.34	$y = 287.19–1.1x$ N:1906 r: –0.76 SE: 0.50	$y = 289.48–1.07x$ N:485 r: –0.57 SE: 0.575
	Forest	$y = 281.735+0.97x$ N: 361 r: 0.49 SE: 0.38	$y = 284.96–0.663x$ N:8863 r: –0.53 SE: 0.573	$y = 286.16–0.10x$ N:1047 r: –0.44 SE: 0.305	No data
	Agriculture	$y = 282.35–1.06x$ N: 82 r: –0.66 SE: 0.900	$y = 284.92–0.10x$ N:433 r: –0.68 SE: 0.531	$y = 286.73–0.42x$ N:3528 r: –0.62 SE: 0.490	$y = 290.94–1.01x$:875 r: –0.473 Std: 0.585

Note: Dependent variable y: LST, land surface temperature; independent variable x: FVC, fractional vegetation cover; N, number of samples; r: correlation coefficient; SE: standard error.

2 and 3. The analyses were based on winter images; however, it can be concluded that the correlation coefficients of LST and FVC would be expected to be higher if summer images were used.

In general, the result shows an inverse correlation relationship with some variations between LST and FVC within the LULC categories of LST zones, and the correlation coefficients associated with LULC categories and LST zones are different. It is known that FVC and NDVI differ due to strong seasonal variation, which may further complicate the relationship of FVC with LST. Thus, the use of FVC to understand urban heat environment should be cautiously done.

3.4. Landscape metrics and LST zones analysis

A key aspect of this study was to examine the relationship between landscape (LULC) patterns and LST through landscape metric analysis. Accordingly, it is noticeable that urban, grassland, and agriculture had changed significantly between 1993 and 2006; the spatial patterns of these three LULC categories were analysed and discussed in detail (Figures 7). In this analysis, the landscape metrics derived from LULC and LST zones were applied to examine the graphic relationships of LULC metrics with the four LST zones derived from the bi-temporal images. As can be implied from Figures 2 and 3 and Table 4, the zonal distribution patterns, represented by the landscape metrics, obviously vary with the different LULC categories and dates (and hence, season and the weather), which has some implications for the LST and LST zone classification. However, there are similar trends in PD and PAFRAC between the two dates (Figure 7). The trends also indicate that zone 1 LST exhibited the lowest PD and PAFRAC values, and then both metrics increased to maximum values in zone 3 or 2, which then decreased in zone 4. This is indicative of the complexity or heterogeneity of landscapes in zones 2 and 3. Moreover, there is a difference between PD and PAFRAC values for LST zones 2 and 3 in 1993 in comparison to these zones in 2006 for the urban and grassland LULC categories. This is less so for agriculture. The reason for the latter is probably due to the fact that agricultural activities involving market gardening that is reliant on irrigation do not vary very much from season to season.

In the case of MPS and AI (Figure 7), their trends in relation to the LST zones are not as clear-cut as is the case with PAFRAC and PD. The trends exhibited by urban are remarkably similar, with only a slight variation in the zonal MPS and AI in 1993, and the 2006 MPS and AI peaking in zone 3. This is probably because urban expansion occurred more in zone 3 than in other zones, in addition to the influence of prevailing weather conditions at the time of image acquisition.

When examining the detailed comparison of each of the metrics of the LST zones for the two dates, starting with urban trends, it is noticeable that urban had higher PD values in zones 2 and 3, although much less so in 2006 compared with the values in 1993, the PD values are close to zero in zones 1 and 4 for the two dates (Figure 7). This means that urban LULC had expanded mainly in zones 2 and 3 and was interspersed with grassland, agriculture, and forest (Figure 2). Urban also had a similar trend in PAFRAC to PD, peaking in zones 2 and 3 and then declining to a value much larger than zero in zones 1 and 4 for both 1993 and 2006, although its decline from 1993 to 2006 is less than was the case for PD. This means that humans had an obvious impact on these landscape zones. In the case of MPS and AI (Figure 7), the two dates had similar trends from zones 1–4. In 1993, both urban MPS and AI were slightly higher in zone 1 and then declined gradually through to zone 4, whereas in 2006, there was a sharp rise in both MPS and AI from zone 2, peaking in zone 3, and declining in zone 4. This indicates that the average area of urban patches

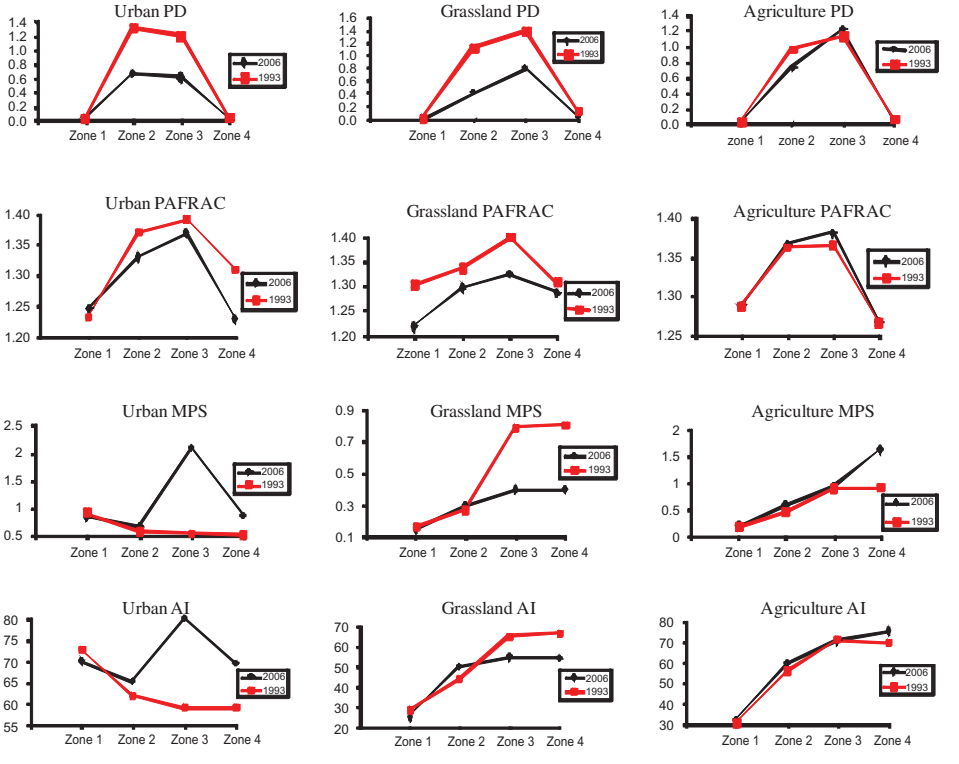

Figure 7. The landscape metrics versus LST zones created from the bi-temporal Landsat images.

in zone 3 obviously increased from much smaller patches in 1993 to larger ones in 2006. As urban PD values for zones 2 and 3 declined between the two dates, urban in zone 3 had been aggregated, which was compensated by the more compact urban patches in zone 4.

Grassland had similar trends in PD and PAFRAC as urban (Figure 7), with both metrics peaking in zone 3. Both had declined in most of the zones from 1993 to 2006. This can be explained by grassland being mainly distributed in a dot pattern interspersed with urban and agriculture, as impacted by human disturbances. Grassland also showed similar change trends in MPS and AI between the two dates (Figure 7). The MPS and AI values in zone 2 of 1993 were lower than those in 2006; in zones 1, 3, and 4, especially in zones 3 and 4, MPS and PD declined from 1993 to 2006, which means that grassland had decreased patch sizes and a smaller number of patches. This may be explained by the fact that the distribution of changes in grassland was due to the changing patterns of LUCC.

Agriculture in the study area had different change trends from urban and grassland. Evidence from Table 3 indicates that agricultural area in peri-urban and in the vicinity had increased from 739.785 km^2 in 1993 to 842.726 km^2 in 2006. The PD and PAFRAC values of agriculture have similar trends for the two dates; it increased and reached the peak in zone 3 and declined to close to zero for PD and just over 1.25 for PAFRAC (Figure 7). The PAFRAC value in zones 3 and 2 increased from 1993 to 2006, but there were no changes in zone 1 (mainly growing crops) and 4 (mainly unplanted bare soil) in the same period. There was hardly any change in the two metrics (PD and PAFRAC) between the two dates. However, while agriculture has a similar trend of MPS across the zones for the two dates, MPS had increased significantly in zone 4 between 1993 and 2006 (Figure 7). This was

hardly the case with AI. By way of explanation, except for urban expansion, the change in agriculture was also influenced by agricultural activities (due to increased irrigation activities and crop area in 2006) and seasonal and weather effects on the LST zones.

4. Discussion and conclusions

LST is one of the key surface parameters in environmental studies. LULC categories are linked to distinct behaviours of the urban thermal environment. In this study, the spatial characteristics of the landscape and LST patches in Sydney were explored using FVC and the interpretation of landscape metrics derived from LULC and LST maps.

Vegetation cover in urban areas reduces the surface radiant temperature, which results in relatively low LST values. The analysis of LST and FVC showed that the vegetation fraction had a significant effect on the urban heat environment and provides the linear correlation recursive equation between LST zones and FVC. It is also noteworthy that the correlation coefficients are different for different LST zones of southwest Sydney. It is also known that FVC is strongly affected by season. The analysis was based on winter images, most likely the correlation coefficients of LST and FVC are expected to be higher if summer images were used. Therefore, further studies are needed to assess the LST over different seasons in order to understand and capture the full picture of the process.

We also analysed the relationship between landscape pattern and LST, which provides a conceptual framework for understanding the dynamics of the urban thermal environment; this is useful for urban environmental management. We have demonstrated that remote-sensing satellite imagery can be used to derive landscape patterns and LSTs and to identify their complicated relationship. Thus, in conjunction with GIS, remote-sensing technology can be applied to determine the location and shape of urban component surfaces, which can be used as background information for urban planners and environmental managers to minimize the negative thermal effects of urban development.

Few studies have used landscape metrics in the analysis of LST and the relationship between landscape and LST patterns. This article has shown the relationship between landscape patterns and LSTs of two-temporal images. The study has shown that with the integration of remote sensing, GIS, and a landscape ecology approach, landscape metrics are effective tools to quantify the landscape and LST patterns. These measurements can provide precise characterization and quantification of the spatial characteristics of urbanization and the urban thermal environment. From the analysis above, the spatial characteristics of landscape metrics and LST can be used to evaluate the urban ecological environment. They can also provide an effective tool for evaluating the environmental influences of zoning in urban ecosystems using remote sensing and GIS.

Landscape metrics are widely used to quantify landscape patterns at different scales. These metrics may be applicable in comparing LULC and LSTs for different urban areas at different times. It is also worth noting that the landscape metrics are sensitive to spatial scales (Turner 1990) and vary with the spatial resolution of satellite images. Choosing proper scales is important for landscape pattern analysis. It may be necessary to determine an appropriate scale prior to the study on interactions between landscape pattern and thermal environment. In this study, the relationship between landscape and LST patterns was based on landscape metrics at 60 m spatial resolution. In future studies, there is the need to focus on the study of the relationship between landscape pattern and thermal environment by multi-scale and multi-resolution analysis.

From the above analysis, the metrics of LST zones appear to correspond to the metrics of LULC categories. This correspondence indicates that the spatial configuration of a

specific temperature zone is closely related to the spatial configuration of dominant LULC categories in that zone. It is known that LULC and LST vary with seasons. Therefore, further studies are required to examine the seasonal impacts on the relationship between LULC pattern and LST, and the impact of the distribution pattern of different LULC categories on the urban landscape.

Acknowledgements

This work was partially funded by the Commonwealth of Australian Endeavour Research Fellowship awarded to the first author. The authors are also grateful to the Fujian Normal University, Fuzhou, for providing study leave, which enabled the first author to be involved with this project. Further acknowledgement goes to reviewers for their constructive comments and suggestions.

References

ABS (Australian Bureau of Statistics). 2003. Glossary of Statistical Geography Terminology, 2003. Government of Australia. Accessed December 21, 2008. http://www.abs.gov.au/AUSSTATS/abs@.nsf/Lookup/6537.0Main+Features12003-04?OpenDocument.

Bain, D. J., and G. S. Brush. 2004. "Placing the Pieces: Reconstructing the Original Property Mosaic in a Warrant and Patent Watershed." *Landscape Ecology* 19: 843–56.

Bender, O., H. H. Boehmer, D. Jens, and K. P. Schumacher. 2005. "Analysis of Land-Use Change in a Sector of Upper Franconia (Bavaria, Germany) Since 1850 Using Land Register Records." *Landscape Ecology* 20: 149–63.

BRS. 2006. *Guidelines for Land Use Mapping in Australia: Principles, Procedures and Definitions*. 3rd ed. Canberra: Bureau of Rural Sciences.

Carlson, T. N., R. R. Gillies, and E. M. Perry. 1994. "A Method to Make Use of Thermal Infrared Temperature and NDVI Measurements to Infer Surface Soil Water Content and Fractional Vegetation Cover." *Remote Sensing Reviews* 9: 161–73.

Carlson, T. N., and S. T. Arthur. 2000. "The Impact of Land Use-Land Cover Changes Due To Urbanization on Surface Microclimate and Hydrology: A Satellite Perspective." *Global and Planetary Change* 25: 49–65.

Chander, G., and B. Markham. 2003. "Revised Landsat-5 TM Radiometric Calibration Procedures and Post-Calibration Dynamic Ranges." *IEEE Transactions on Geoscience and Remote Sensing* 41: 2674–7.

Che, N., and J. C. Price. 1992. "Survey of Radiometric Calibration Results and Methods for Visible and Near-Infrared Channels of NOAA-7, -9 and -11 AVHRRs." *Remote Sensing of Environment* 41: 19–27.

Chen, X. L., M. Z. Zhao, P. X. Li, and Z. Y. Yin. 2006. "Remote Sensing Image-Based Analysis of the Relationship between Urban Heat Island and Land Use/Cover Changes." *Remote Sensing of Environment* 104: 133–46.

Frohn, R., and Y. Hao. 2006. "Landscape Metric Performance in Analyzing Two Decades of Deforestation in the Amazon Basin of Rondonia, Brazil." *Remote Sensing of Environment* 100: 237–51.

Gallo, K. P., A. L. Mcnab, T. R. Karl, J. F. Brown, J. J. Hood, and J. D. Tarpley. 1993. "The Use of a Vegetation Index for Assessment of the Urban Heat Island Effect." *International Journal of Remote Sensing* 14: 2223–30.

Gallo, K. P., and T. W. Owen. 1999. "Satellite-Based Adjustment for the Urban Heat Island Temperature Bias." *Journal of Applied Meteorology* 38: 806–13.

Gillies, R. R., T. N. Carlson, J. Cui, W. P. Kustas, and K. S. Humes. 1997. "A Verification of the 'Triangle' Method for Obtaining Surface Soil Water Content and Energy Fluxes from Remote Measurements of the Normalized Difference Vegetation Index (NDVI) and Surface Radiant Temperature." *International Journal of Remote Sensing* 18: 3145–66.

Goward, S. N. 1981. "Thermal Behavior of Urban Landscapes and the Urban Heat Island." *Physical Geography* 2: 19–33.

Gustafson, E. J. 1998. "Quantifying Landscape Spatial Pattern: What Is the State of the Art?" *Ecosystems* 1: 143–56.

Haines-Young, R., and M. Chopping. 1996. "Quantifying Landscape Structure: A Review of Landscape Indices and Their Application to Forested Landscapes." *Progress in Physical Geography* 20: 418–45.

He, H. S., B. E. DeZonia, and D. J. Mladenoff. 2000. "An Aggregation Index (AI) to Quantify Spatial Patterns of Landscapes." *Landscape Ecology* 15: 591–601.

Kato, S., and Y. Yamaguchi. 2007. "Estimation of Storage Heat Flux in an Urban Area Using ASTER Data." *Remote Sensing of Environment* 110: 1–17.

Liu, H., and Q. Weng. 2008. "Seasonal Variations in the Relationship between Landscape Pattern and Land Surface Temperature in Indianapolis, USA." *Environmental Monitoring and Assessment* 144: 199–219.

Liu, H., and Q. Weng. 2009. "An Examination of the Effect of Landscape Pattern, Land Surface Temperature, and Socioeconomic Conditions on WNV Dissemination in Chicago." *Environmental Monitoring and Assessment* 159: 143–161.

McGarigal, K., and B. J. Marks. 1995. FRAGSTATS: *Spatial Pattern Analysis Program for Quantifying Landscape Structure.* General Technical Report PNW-GTR-351. Portland, OR: USDA, Forest Service, Pacific Northwest Research Station.

McPherson, E. G., D. Nowak, G. Heisler, S. Grimmond, C. South, R. Grant, and R. Rowntree. 1997. "Quantifying Urban Forest Structure, Function, and Value: The Chicago Urban Forest Climate Project." *Urban Ecosystems* 1: 49–61.

Nichol, J. E. 1996. "High-Resolution Surface Temperature Patterns Related to Urban Morphology in a Tropical City: A Satellite-Based Study." *Journal of Applied Meteorology* 28: 276–84.

O'Neill, R. V., J. R. Krummel, R. H. Gardner, G. Sugihara, B. Jackson, D. L. DeAngelis, B. T. Milne, et al. 1988. "Indices of Landscape Pattern." *Landscape Ecology* 1: 153–62.

Owen, T. W., T. N. Carlson, and R. R. Gillies. 1998. "An Assessment of Satellite Remotely Sensed Land Cover Parameters in Quantitatively Describing the Climatic Effect of Urbanization." *International Journal of Remote Sensing* 19: 1663–81.

Pan, D., G. Domon, D. Marceau, and A. Bouchard. 2001. "Spatial Pattern of Coniferous and Deciduous Forest Patches in an Eastern North America Agricultural Landscape: The Influence of Land Use and Physical Attributes." *Landscape Ecology* 16: 99–110.

Peña, M. 2008. "Relationships between Remotely Sensed Surface Parameters Associated with the Urban Heat Sink Formation in Santiago, Chile." *International Journal of Remote Sensing* 29: 4385–404.

Price, J. C. 1987. "Calibration of Satellite Radiometers and the Comparison of Vegetation Indices." *Remote Sensing of Environment* 21: 15–27.

Qin, Z., and A. Karnieli. 1999. "Progress in the Remote Sensing of Land Surface Temperature and Ground Emissivity Using NOAA–AVHRR Data." *International Journal of Remote Sensing* 20: 2367–93.

Quattrochi, D. A., and M. K. Ridd. 1998. "Analysis of Vegetation within a Semi-Arid Urban Environment Using High Spatial Resolution Airborne Thermal Infrared Remote Sensing Data." *Atmosphere Environment* 32: 19–33.

Riitters, K. H., R. V. O'Neill, C. T. Hunsaker, J. D. Wickham, D. H. Yankee, S. P. Timmins, K. B. Jones, B. L. Jackson. 1995. "A Factor Analysis of Landscape Pattern and Structure Metrics." *Landscape Ecology* 10: 23–39.

Sandholt, I., K. Rasmussen, and J. Andersen. 2002. "A Simple Interpretation of the Surface Temperature/Vegetation Index Space for Assessment of Surface Moisture Status." *Remote Sensing of Environment* 79: 213–24.

Smith, R. M. 1986. "Comparing Traditional Methods for Selecting Class Intervals on Choropleth Maps." *Professional Geographer* 38: 62–7.

Smith, S. 2003. "Population Growth: Implications for Australia and Sydney." NSW Parliamentary Library Research Service, Briefing Paper 5/03.

Snyder, W. C., Z. Wan, Y. Zhang, and Y. Z. Feng. 1998. "Classification Based Emissivity for Land Surface Temperature Measurement from Space." *International Journal of Remote Sensing* 19: 2753–74.

Turner, M. G. 1990. "Spatial and Temporal Analysis of Landscape Patterns." *Landscape Ecology* 4: 21–30.

Turner, M. G., R. H. Gardner, and R. V. O'Neill. 2001. *Landscape Ecology. Theory and Practice: Pattern and Process*. New York: Springer-Verlag.

Turner, R. E., N. N. Rabalais, D. Justic, and Q. Dortch. 2003. "Global Patterns of Dissolved N, P and Si in Large Rivers." *Biogeochemistry* 64: 297–317.

Vinnikov, K. Y., Y. Yu, M. K. Rama Varma Raja, D. Tarpley, and M. D. Goldberg. 2008. "Diurnal-Seasonal and Weather-Related Variations of Land Surface Temperature Observed from Geostationary Satellites." *Geophysical Research Letters* 35: L22708. doi:10.1029/2008GL035759.

Voogt, J. A., and T. R. Oke. 1997. "Complete Urban Surface Temperatures." *Journal of Applied Meteorology* 36: 1117–32.

Voogt, J. A., and T. R. Oke. 2003. "Thermal Remote Sensing of Urban Climates." *Remote Sensing of Environment* 86: 370–84.

Wan, Z., and J. Dozier. 1996. "A Generalized Split-Window Algorithm for Retrieving Land-Surface Temperature from Space." *IEEE Transactions on Geoscience and Remote Sensing* 34: 892–905.

Weng, Q. 2003. "Fractal Analysis of Satellite-Detected Urban Heat Island Effect." *Photogrammetric Engineering and Remote Sensing* 69: 555–65.

Weng, Q., D. Lu, and J. Schubring. 2004. "Estimation of Land Surface Temperature-Vegetation Abundance Relationship for Urban Heat Island Studies." *Remote Sensing of Environment* 89: 467–83.

Wilson, A. K. 1988. "The Effective Resolution Element of Landsat Thematic Mapper." *International Journal of Remote Sensing* 9: 1303–14.

Wilson, J. S., M. Clay, E. Martin, D. Stuckey, and K. V. Risch. 2003. "Evaluating Environmental Influence of Zoning in Urban Ecosystems with Remote Sensing." *Remote Sensing of Environment* 86: 303–21.

Wittich, K. P., and O. Hansing. 1995. "Area-Averaged Vegetative Cover Fraction Estimated from Satellite Data." *International Journal of Biometeorology* 38: 209–15.

Woodcock, C. E., and A. H. Strahler. 1987. "The Factor of Scale in Remote Sensing." *Remote Sensing of Environment* 21: 311–22.

Wu, J., E. J. Dennis, L. Matt, and T. T. Paul. 2000. "Multiscale Analysis of Landscape Heterogeneity: Scale Variance and Pattern Metrics." *Geographic Information Sciences* 6: 6–19.

Xian, G., and M. Crane. 2006. "An Analysis of Urban Thermal Characteristics and Associated Land Cover in Tampa Bay and Las Vegas Using Landsat Satellite Data." *Remote Sensing of Environment* 104: 147–56.

Yuan, F., and M. Bauer. 2007. "Comparison of Impervious Surface Area and Normalized Difference Vegetation Index as Indicators of Surface Urban Heat Island Effects in Landsat Imagery." *Remote Sensing of Environment* 106: 375–86.

Yue, W., J. Xu, W. Tan, and L. Xu. 2007. "The Relationship between Land Surface Temperature and NDVI with Remote Sensing: Application to Shanghai Landsat 7 ETM+ Data." *International Journal of Remote Sensing* 28: 3205–26.

Zhang, Y., I. Odeh, and C. Han. 2009. "Bi-Temporal Characterization of Land Surface Temperature in Relation to Impervious Surface Area, NDVI and NDBI, Using a Sub-Pixel Image Analysis." *International Journal of Applied Earth Observation and Geoinformation* 11: 256–64.